

# Analysis of Synthetic Flames

Stephanie A. Coronel<sup>1</sup>, Rémy Mével<sup>2,3</sup>, Joseph E. Shepherd<sup>1</sup>

<sup>1</sup>California Institute of Technology, Pasadena, CA, USA

<sup>2</sup>Center for Combustion Energy, <sup>3</sup>Dept. of Automotive Engineering, Tsinghua University

## 1 Introduction

Laminar flame properties such as the laminar burning speed and the Markstein length are important fundamental parameters for a wide number of combustion applications. The laminar burning speed is defined as the normal propagation velocity of fresh gas relative to a fixed, planar flame front; it is frequently measured experimentally using spherically expanding flames [1]. The presence of flame stretch in such experiments precludes direct measurement of the laminar flame speed [2]. Instead, the measured flame speed has to be extrapolated to conditions of zero stretch. [3] first proposed this correction to the burning speed by introducing a parameter known as the Markstein length which characterizes the response of the flame to stretch. Asymptotic theoretical analysis [4, 5, 6] performed in the limit of high activation energy and low stretch rate have related the stretched and unstretched burning speeds through a linear relationship. Further theoretical work by [4] has led to a nonlinear relationship between the stretched and the unstretched burning speed which has been used by a number of groups in the past few years to account for nonlinear effects of stretch on the flame propagation. Comparison of the results obtained through linear and nonlinear extrapolations demonstrated that both the burning speed and Markstein length can be poorly estimated by the linear method for mixtures that are away from stoichiometry [7, 8]. The present work discusses the performance of nonlinear fitting methods by extracting the laminar flame properties from synthetic data sets. The sensitivity of the results to experimental parameters like initial and final flame radius, the number of points in the data set, and measurement noise, as well as numerical parameters like the initial guess that is used to start the nonlinear fit, are investigated.

## 2 Methodology

Using asymptotic methods based on large activation energy, [4] obtained a nonlinear model for spherical flame speed as a function of curvature (Eq. 1).

$$\left(\frac{S_b}{S_b^0}\right)^2 \ln\left(\frac{S_b}{S_b^0}\right) = -2\frac{L_B\kappa}{S_b^0}. \quad (1)$$

This expression can be used to derive the unstretched flame speed and the Markstein length. One approach to doing this is to analyze the flame radial time history  $R_f = f(t)$  data by fitting it to polynomials and differentiating to determine  $S_b = dR_f/dt$  [8? ]. Numerical differentiation of the experimental data leads

to amplification of existing noise. To avoid differentiating the experimental data, [7] proposed an integrated form of Eq. 1. In the present study, numerical integration rather than analytic integration is used for extracting the flame properties from the nonlinear model of [4].

### 3.1 Extracting Flame Properties

Equation 1 has unknowns  $S_b^0$  and  $L_B$  for a given  $R_f$  and  $S_b = dR_f/dt$ . The data,  $R_f = f(t)$ , can be synthetically generated or obtained from an experiment. To avoid numerical differentiation of  $R_f$  to obtain  $S_b$ , Eq. 1 is numerically integrated using the Matlab implicit ode solver `ode15i` using an initial set of guesses for  $S_b^0$  and  $L_B$ . The integration yields a solution,  $R_f^{\text{trial}}$ , that is used to compute an objective function,

$$\text{Error} = \sum_{i=0}^N [R_{f,i} - R_{f,i}^{\text{trial}}(\vec{a}, t_i)]^2, \quad (2)$$

where  $\vec{a} = \{L_B, S_b^0\}$ . The values of  $L_B$  and  $S_b^0$  are iteratively refined by minimizing the objective function, Eq. 2, using the Levenberg-Marquardt algorithm implemented in the Matlab nonlinear least squares solver, `lsqnonlin`.

Previous studies [7, 8] investigated the accuracy of the linear and nonlinear methods by using experimental data to extract flame properties. However, the exact unstretched flame speed and Markstein length were not known a priori and the two methods (linear vs. nonlinear) yielded different results. The approach of [9] used synthetic data generated through unsteady 1-D numerical simulations performed with detailed chemistry. In the performance studies of the present nonlinear approach, synthetic data is generated by numerically integrating the Ronney-Sivashinsky expression to obtain the flame radius as a function of time. This is accomplished by implicitly integrating Eq. 3 (Eq. 1 rewritten in terms of  $R_f$ ) for a set of  $L_B$  and  $S_b^0$  values.

$$\frac{dR_f/dt}{S_b^0} \cdot \ln\left(\frac{dR_f/dt}{S_b^0}\right) = -2\frac{L_B}{R_f} \quad (3)$$

Different levels of Gaussian noise are added to the solution  $R_f$  to simulate the noise present in experimental data. Consequently, the present study assumes that the dynamics of the spherically expanding flame can be perfectly described by Eq. 3. As discussed in previous studies [10, 11, 12], Eq. 3 is not an exact model for the propagation of realistic flames (experimental or from 1-D simulations) and other linear or nonlinear models of flame propagation could be employed [11].

## 4 Performance of Methodology

The proposed nonlinear fitting method minimizes the objective function given by Eq. 2. The rate of convergence, sensitivity to noise, and robustness of this procedure depends on the minimization method and the behavior of the objective function. An example of the objective function is shown in Fig. 1 (a); the contour plot is created by generating synthetic data points of flame radius vs. time for a test case ( $L_B = -1$  mm and  $S_b^0 = 2.5$  m/s) and then evaluating Eq. 2 at different values of the Markstein length and unstretched flame speed. The minimum error occurs over the correct solution point; however, the objective function contours are elongated, indicating that the solution point is much less sensitive to the Markstein length than to the unstretched flame speed. The elongated shape of the minimum in the objective function is also a property of

the linear method:  $S_b = S_b^0 - L_B \kappa$ . Contours of the objective function obtained through the linear method are shown in Fig. 1 (b). The qualitative behavior of the two methods is similar; however, the minimum for the linear method deviates from the actual solution of  $L_B = -1$  mm and  $S_b^0 = 2.5$  m/s since the flame characteristics lie slightly outside of the linear stretch regime.

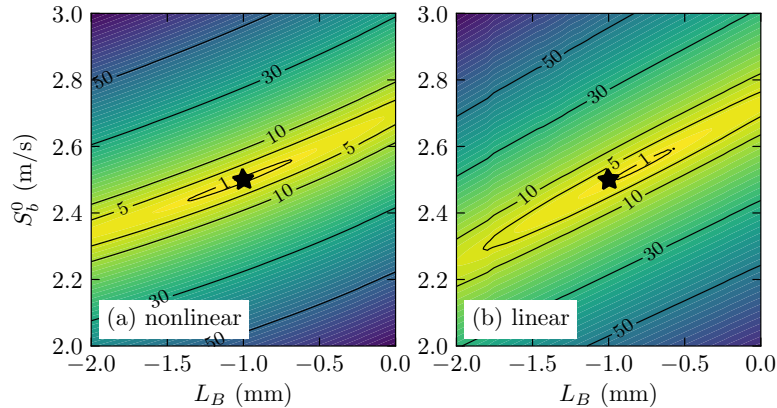


Figure 1: Contour plots of the objective function; the actual solution (indicated by the filled black star) is  $L_B = -1$  mm,  $S_b^0 = 2.5$  m/s.

The minimum error at each Markstein length is shown in Fig. 2 for different levels of Gaussian noise added to the test case. The objective function exhibits a global minimum at the correct solution, but the depth of the minimum and the slope in its vicinity decrease when noise is added. For noise levels of 1% and 2%, the minimum is shallow and is shifted to more negative Markstein lengths. Other noise models have been employed, including uniform noise and noise that decreases with increasing flame radius; the results from those models are nearly indistinguishable from those shown in Fig. 2.

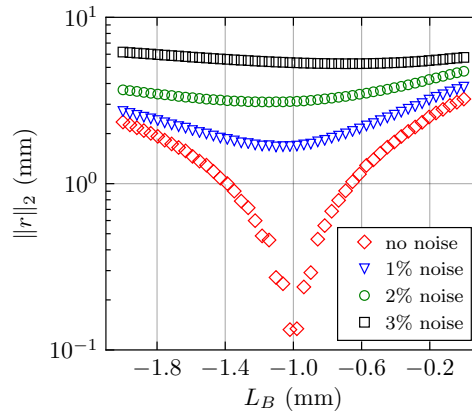


Figure 2: Minimum error values for range of  $S_b^0$  as a function of  $L_B$ ; the actual solution is  $L_B = -1$  mm and  $S_b^0 = 2.5$  m/s; random Gaussian noise has been included by adding 1%, 2%, and 3% relative error to each flame radius point.

#### 4.1 Performance Parameters

To evaluate the performance of the minimization method, synthetic  $R_{f,i}$  vs.  $t_i$  data with added Gaussian noise are generated using Eq. 3 for  $L_B \in [-5.0, L_{B,\max}]$  mm where  $L_{B,\max} = R_{f,0}/2e$  and  $S_b^0 \in [0.3, 35]$  m/s; the range of  $L_B$  and  $S_b^0$  values are representative of flame properties for typical hydrocarbon-air and hydrogen-air mixtures (although not all the combinations of  $L_B$  and  $S_b^0$  can be physically observed for real mixtures). The choice of  $L_{B,\max}$  is based on the intrinsic limit of Eq. 1. After generating the data, an attempt is made to recover the laminar flame parameters from the synthetic data using a set of initial guesses for  $L_B$  and  $S_b^0$ . The performance of the present method is evaluated by varying the range of  $R_f$ , the size of the data set, i.e.  $|R_f|$ , and the added Gaussian noise. The performance of the method is quantified in terms of the uncertainty and variance of the fitted values of  $L_B$  and  $S_b^0$ . The uncertainty for  $\vec{a}$  is found by extracting the Jacobian,  $J_{ik}$ , using the Matlab function `lsqnonlin` where

$$J_{ik}^2 = \left. \frac{\partial^2 r_i}{\partial a_k^2} \right|_{\vec{a}^*} \quad \text{and} \quad r_i = R_{f,i} - R_{f,i}^{\text{trial}}(\vec{a}^*, t_i), \quad (4)$$

$\vec{a}^*$  is the vector of parameters giving the best fit. The uncertainty is then given by,

$$\Delta \vec{a}_k = \left[ 3 \sum_i \Delta R_{f,i}^2 / \sum_i J_{ik}^2 \right]^{1/2}, \quad (5)$$

where  $\Delta R_{f,i}$  is the uncertainty in the  $i^{\text{th}}$  data point and  $\Delta \vec{a} = \{\Delta L_B, \Delta S_b^0\}$ . The variance,  $\sigma^2$ , of the Markstein length and the unstretched flame speed is found by sampling each combination of  $L_B$  and  $S_b^0$  one hundred times. The samples for an individual combination are then fitted to a Gaussian distribution,

$$\phi(\vec{a}^*, \vec{\sigma}, \vec{\mu}) = \frac{1}{\vec{\sigma} \sqrt{2\pi}} \exp\left(-\frac{(\vec{a}^* - \vec{\mu})^2}{2\vec{\sigma}^2}\right), \quad (6)$$

to estimate the standard deviation,  $\vec{\sigma}$ , and the mean,  $\vec{\mu}$ .

#### 4.2 Parametric Study

The performance of the present method is evaluated by varying: the data set size of  $R_f$  from 10 to 100 points, the data set range  $R_f = [R_{f,0}, R_{f,N}]$  where  $R_{f,N} = \{25, 38, 58, 70\}$  mm, and the level of Gaussian noise added to  $R_f$ . Several examples of results obtained by varying the Gaussian noise level are discussed in this section. The calculated  $L_B$  for a combination of  $L_B \in [-5.0, L_{B,\max}]$  mm and  $S_b^0 = 0.3$  m/s is shown in Fig. 3 for (a) 10% and (b) 1% Gaussian noise; the uncertainty bands calculated through Eq. 5 are shown by the shaded region and the actual result is indicated by the black line. Figure 3 (a) indicates that data with 10% Gaussian noise will yield highly uncertain calculations of the Markstein length ( $\sigma = \pm 1.44$  mm (29%) for  $L_B = -5$  mm and  $\sigma = \pm 0.5$  mm (29%) for  $L_B = 1.7$  mm); however, the results will have the appropriate uncertainty bounds since the true value, shown by the black line, lies within the uncertainty band, shown by the shaded regions. Figure 3 (b) shows that the calculations are clustered around the actual result (black line); the corresponding standard deviation results are,  $\sigma = \pm 0.46$  mm (9%) for  $L_B = -5$  mm and  $\sigma = \pm 0.17$  mm (10%) for  $L_B = 1.7$  mm.

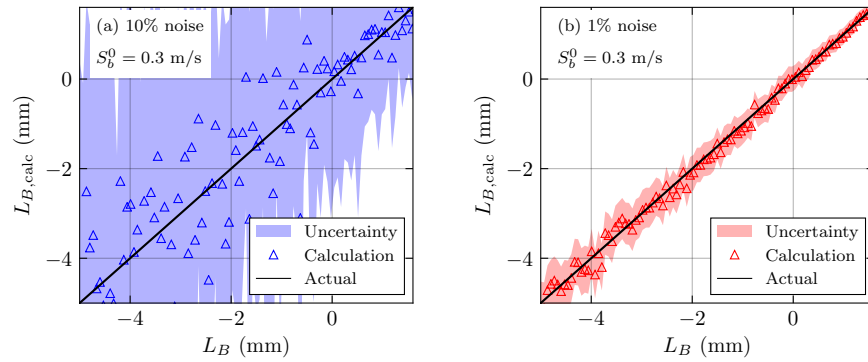


Figure 3: Effect of Gaussian noise on calculation of  $L_B$  for  $R_f = [10, 58]$  mm,  $|R_f| = 100$ ,  $S_b^0 = 0.3$  m/s, and (a) 10% and (b) 1% Gaussian noise.

The calculated  $S_b^0$  for a combination of  $S_b^0 \in [0.3, 35]$  m/s and  $L_B = -5.0$  mm is shown in Fig. 4 for (a) 10% and (b) 1% Gaussian noise. Figure 4 (a) shows similar behavior to that observed in the uncertainty of  $L_B$ ; 10% Gaussian noise will yield uncertain calculations of the unstretched flame speed ( $\sigma = \pm 0.55$  m/s (13%) for  $S_b^0 = 4.15$  m/s and  $\sigma = \pm 1.70$  mm (5%) for  $S_b^0 = 35$  m/s). Added Gaussian noise of 1% (shown in Fig. 4 (b)) will yield less uncertain calculations of the unstretched flame speed ( $\sigma = \pm 0.17$  m/s (4%) for  $S_b^0 = 4.15$  m/s and  $\sigma = \pm 0.52$  mm (1%) for  $S_b^0 = 35$  m/s).

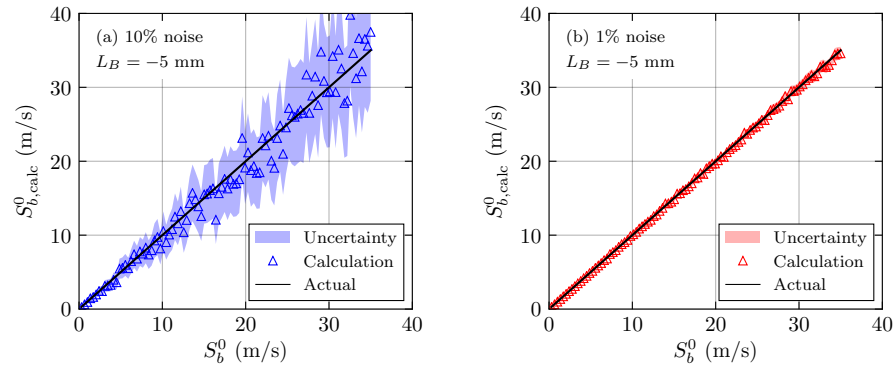


Figure 4: Effect of Gaussian noise on calculation of  $S_b^0$  for  $R_f = [10, 58]$  mm,  $|R_f| = 100$ ,  $L_B = -5.0$  mm, and (a) 10% and (b) 1% Gaussian noise.

By varying the data set size, range, and noise level over the range of  $L_B$  and  $S_b^0$  tested, the parametric study suggests that at least 50 points are needed in the data set, i.e. flame radius vs. time, and a minimum flame radius range of 48 mm to obtain standard deviations on the order of 1% for the unstretched flame speed and 10% for the Markstein length.

## 5 Conclusion

Laminar burning speed and Markstein length are important quantities to validate chemical reaction mechanisms and model turbulent combustion. The development of asymptotic theories to account for stretch

effects has considerably reduced the scatter in experimental flame measurements [1]. The linear extrapolation method has been extensively used but its applicability is limited to mixtures which exhibit weak sensitivity to stretch, roughly for  $L_B \in [-1.0, 1.0]$  mm. For mixtures which are more sensitive to stretch, away from the stoichiometry, the nonlinear extrapolation method, which employs the Ronney-Sivashinsky (R-S) equation, appears to give more reliable results. The R-S equation exhibits a strong sensitivity to the properties of the  $R_f = f(t)$  data set. In order to determine the flame speed and Markstein length with accuracy and minimize the uncertainty, the present results indicate that the experiments should result in data with a large number of points ( $> 50$ ), a large flame radius range ( $> 48$  mm), and low noise.

## References

- [1] Egolfopoulos FN, Hansen N, Ju Y, Kohse-Hoinghaus K, Law CK, Qi F. (2014). Advances and challenges in laminar flame experiments and implications for combustion chemistry. *Prog. Energ. Combust.* 43: 36.
- [2] Dowdy DR, Smith DB, Taylor SC, Williams A. (1990). The use of expanding spherical flames to determine burning velocities and stretch effects in hydrogen/air mixtures. *P. Combust. Inst.* 23: 325.
- [3] Markstein GH. (1951). Experimental and theoretical studies of flame front instability. *J Aeronaut. Sci.* 18: 199.
- [4] Ronney PD, Sivashinsky GI. (1989). A theoretical study of propagation and extinction of nonsteady spherical flame fronts. *SIAM J. Appl. Math.* 49: 1029.
- [5] Matalon M, Matkowsky BJ. (1982). Flames as gasdynamic discontinuities. *J. Fluid Mech.* 124: 239.
- [6] Clavin P. (1985). Dynamic behavior of premixed flame fronts in laminar and turbulent flows. *Prog. Energ. Combust.* 11: 1.
- [7] Kelley AP, Law CK. (2009). Nonlinear effects in the extraction of laminar flame speeds from expanding spherical flames. *Combust. Flame.* 156: 1844.
- [8] Halter F, Tahtouh T, Mounaïm-Rousselle C. (2010). Nonlinear effects of stretch on the flame front propagation. *Combust. Flame.* 157: 1825.
- [9] Chen Z. (2011). On the extraction of laminar flame speed and Markstein length from outwardly propagating spherical flames. *Combust. Flame.* 158: 291.
- [10] Wu F, Liang W, Chen Z, Ju Y, Law CK. (2015). Uncertainty in stretch extrapolation of laminar flame speed from expanding spherical flames. *P. Combust. Inst.* 35(1): 663.
- [11] Jayachandran J, Lefebvre A, Zhao R, Halter F, Varea E, Renou B, Egolfopoulos FN (2015). A study of propagation of spherically expanding and counterflow laminar flames using direct measurements and numerical simulations. *P. Combust. Inst.* 35(1): 695.
- [12] Varea E, Beeckmann J, Pitsch H, Chen Z, Renou B. (2015). Determination of burning velocities from spherically expanding  $H_2$ /air flames. *P. Combust. Inst.* 35(1): 711.